

Tritium Management Approach for FHRs Using Supercritical Steam, Open-Air Brayton, and Closed Gas Brayton Power Cycles

Mitchell Atlas, Nick Brickner, Weicheng Chen, Daniel Tsai
Department of Nuclear Engineering

Acknowledgements:

P. F. Peterson, A. Cisneros, L. Huddar
Department of Nuclear Engineering
E. Summerson
Department of Mechanical Engineering

University of California, Berkeley

5/5/2012

Report UCBTH-12-006

ABSTRACT

This project performed a comprehensive analysis of the transport, recovery, and release of tritium in Fluoride Salt-Cooled High Temperature Reactors (FHR) to compare the performance of three different power conversion options: an open air Brayton combined cycle, a supercritical steam Rankine cycle, and a closed gas Brayton cycle. The FHR is a high-temperature, pebble-bed reactor which is cooled by liquid lithium-beryllium fluoride salt. Though the salt provides excellent heat transfer properties, the neutron irradiation of beryllium and lithium produces tritium in comparatively large quantities, posing a potential radiation hazard to plant operators and the environment. By reviewing the existing literature and applying neutronic and mass-transport analysis to the current design, this study intends to model the flow of tritium throughout the FHR system and to suggest potential solutions to improve its extraction and handling.

CONTENTS

Report UCBTH-12-006	1
1.0 INTRODUCTION	3
1.1 Tritium	3
2.0 TRITIUM PRODUCTION	3
2.1 Relevant Reactions	3
2.2 FHR Tritium Production Rate	4
2.3 Tritium Production Rates.....	5
3.0 TRITIUM TRANSPORT	6
3.1 Choices of Coolant/Working Fluid	6
3.2 Components.....	6
3.3 Power Cycles	7
3.4 Tritium Transport Model	8
4.0 TRITIUM PROCESSING	11
4.1 Dose Restrictions.....	12
4.2 Helium Sparging	12
5.0 SUMMARY	15
6.0 REFERENCES.....	16
7.0 APPENDIX.....	18
7.1 MATLAB Code	18

1.0 INTRODUCTION

The three primary options for power conversion for fluoride-salt cooled high temperature reactors (FHRs) involve steam cycles, open air cycles, and closed gas cycles, each of which will have very different issues for tritium management. This project developed and reviewed technical approaches for controlling tritium for each of these power conversion methods, and compares potential FHR tritium releases to those associated with pressurized water reactors (PWRs) and CANDU reactors.

1.1 Tritium

Tritium is the lightest radioactive isotope of hydrogen, comprised of a single proton and two neutrons, with a half-life of 12.32 years. Tritium beta-minus decays into Helium-3 plus one beta-particle (free electron) and electron-antineutrino ($Q=18.6$ keV). Tritium is an unusually low-energy beta emitter with an average kinetic energy of the beta-particle equal to 5.69 keV [10]. Detection of this radioactivity is difficult and requires a liquid scintillation counter which can be in the range of 30% efficient for this low-energy beta decay. The associated beta has an average range in air of only 6.0 mm and is only an internal radiation hazard since penetration of the dead layer of human skin is not possible. As an internal radiation hazard, inhalation and ingestion are the most common hazards but tritium can also combine with oxygen as tritiated water (THO or T_2O) which is absorbable by the skin through the pores.

2.0 TRITIUM PRODUCTION

Tritium is produced in the core of the FHR, so in order to characterize the source of the tritium, its production processes in the core must be studied. MCNP coupled with ORIGEN, or other similar neutronic and depletion analysis codes can be applied to characterize tritium production with varying core power, geometry, temperature, fuel composition and coolant salt composition. The results will depend upon whether the salt is new and still contains residual Li-6 from its initial enrichment, or has reached its equilibrium Li-6 concentration where production of Li-6 from neutron reactions with beryllium is balanced by consumption. These estimates can be compared to experimental values from the literature in order to estimate the rate of tritium production during normal reactor operations immediately after initial startup as well as after sustained operation. Design/operation modifications can then be suggested in order to minimize tritium production without significantly affecting core output.

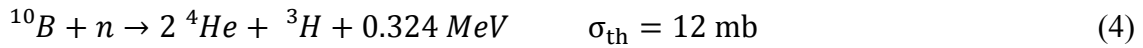
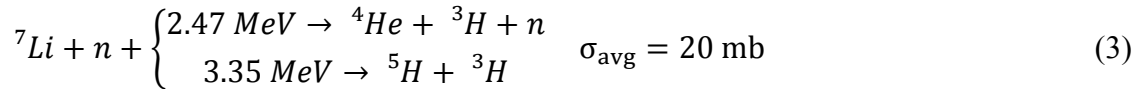
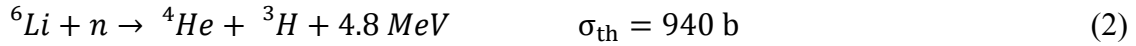
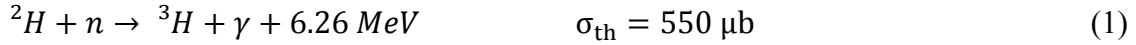
2.1 Relevant Reactions

Tritium is a product of ternary fission reactions in the fuel. Its primary production occurs via neutron induced reactions on deuterium, lithium-6, lithium-7, and boron-10 which can be found in cooling and control elements of various reactor designs.

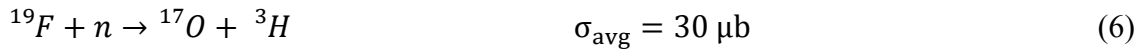
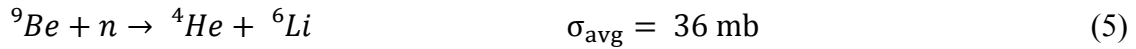
For heavy-water moderated CANDU reactors, the primary production occurs via neutron capture on deuterium in the heavy water moderator. The cross section for this reaction is relatively small, however, the enormous supply of heavy water sufficiently compensates as a rate determining factor. The primary production in PWRs occurs in the boric acid of the reactor coolant system, while in boiling water reactors (BWRs)

production occurs primarily in solid control absorbers, by means of neutron absorption on boron-10.

PWRs also use enriched lithium hydroxide to control pH, which can produce tritium by absorption of a neutron on either lithium-6 or lithium-7. Equations 1-4 list the relevant reactions for CANDU, PWR, and BWR reactors.



In FHRs, the primary means of tritium production occurs in the primary coolant salt. For an FHR using flibe (Li_2BeF_2) as the cooling salt, neutron absorption on beryllium-9, shown in equation 5, serves as the production term of lithium-6 which, when coupled with equation 2, results in a steady-state production of tritium for the life of the reactor. As mentioned before, equation 3 remains relevant, and equation 6 accounts for additional production of tritium by reactions on fluoride in the salt.



2.2 FHR Tritium Production Rate

Figure 1 shows a representative 900 MWth FHR core design [7]. This FHR full-core was modeled using MCNP, and the simulation was simplified using an infinite-core representation by invoking reflective boundary conditions in the axial direction. The pebble-to-coolant volume ratio is 1.5, which reproduces the 40% void fraction generated by random pebble packing, but using a face-centered-cubic pebble lattice to simplify the simulation. Eight depletion regions were modeled with appropriately varying pebble compositions. Though tritium production occurs in the fuel pebbles by ternary fission, this tritium will not escape the pebbles at any significant rate, so the fission source term may be neglected. As a result, the only other source term to account for is neutron capture on lithium in the coolant salt. One further simplification is that at steady-state conditions, the consumption of lithium is balanced by its production by neutron capture on beryllium-9. At steady-state, the concentrations of lithium-6 and lithium-7 in the coolant salt are invariant with time. The essential assumption associated with this Monte Carlo model is that no transients are expected or reflected by the simulation.

The production term requested by MCNP was implemented using a F4 tally. This tally specified the 105 (n,t) reactions in the coolant region. The raw result from MCNP

returned a production term of 1.06408×10^{-4} H-3 per source neutron which is normalized to the power of the reactor. In order to calculate the true production term in our core, this result must be first multiplied by the average neutron generation yield ($\text{nubar}=2.631$), multiplied by the thermal power of the reactor (900 MWt), and divided by the average energy released per fission (200 MeV). The final result of this calculation is a tritium production rate of $7.864 \times 10^{-15} \text{ s}^{-1}$, or 32.8 Ci/day. This value agrees with the literature for the comparable AHTR (2400 MWt) but is lower by almost a factor of 6 [1]. As demonstrated by the AHTR, a 2400-MWt FHR has potential beginning of life and steady-state production rates of approximately 5000 Ci/day (1.8 MCi/yr) and 500 Ci/day, respectively; therefore, based on the results from the AHTR experiment, steady-state production in the primary coolant is approximately 10 times lower than for new coolant. For now, the calculated production term for steady-state conditions will suffice for determining the relative effectiveness of implementing a tritium extraction system.

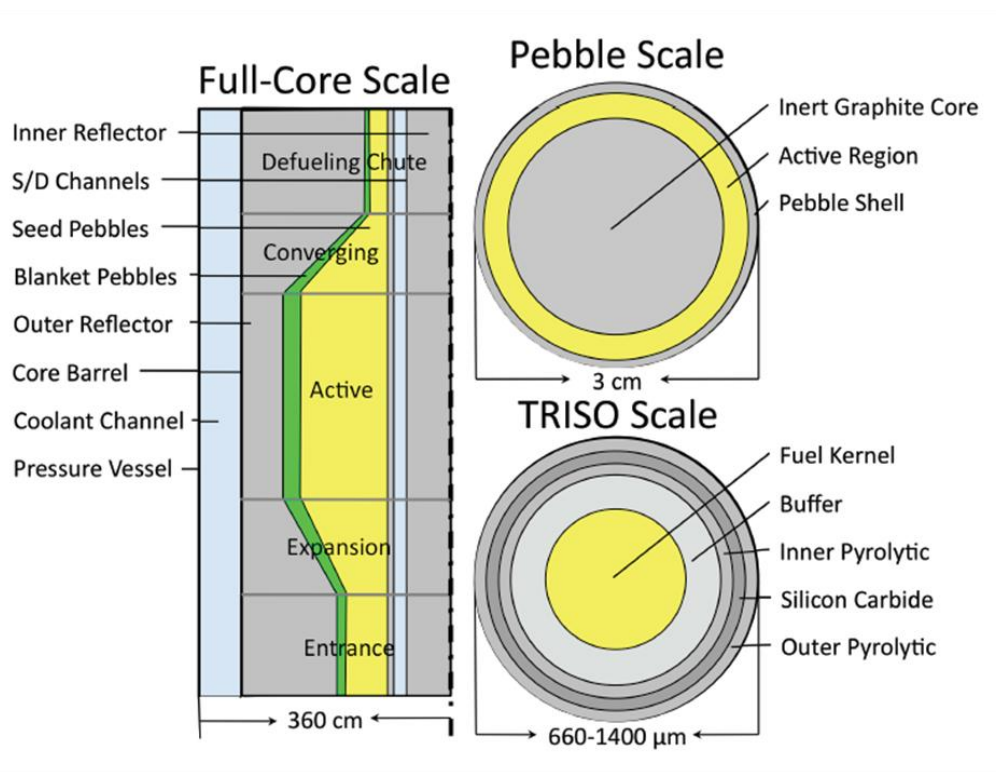


Fig. 1 The FHR full-core, pebble, and TRISO particle representations

2.3 Tritium Production Rates

A 1,000-MWe PWR produces approximately 700 Ci/yr of tritium [13]. BWRs produce about 90% less tritium than PWRs because they do not use soluble boric acid in their primary coolant, and tritium produced in their control blades remains largely immobilized. A 1000-MWe CANDU produces approximately 1 MCi/yr of tritium [5]. The modeled production rate using MCNP for the 900 MWt FHR is 12 kCi/yr; therefore, assuming 40% efficiency, this would mean that a 1,000-MWe FHR would produce approximately 33 kCi/yr at equilibrium. Based on these results, it appears that FHRs

produce approximately 100 times more tritium per MWe than PWRs and 100 times less than CANDU reactors.

3.0 TRITIUM TRANSPORT

Tritium produced in a FHR core is transported throughout the system, and eventually into the surrounding environment through the fluid loops consisting of the primary and intermediate coolant loops as well as the final power conversion cycle. Mass-transfer analyses can be performed on these systems to predict tritium diffusion, solubility, and permeation through solid components as a function of temperature, pressure, compositions and flow conditions. The goal is not necessarily to minimize tritium solubility and diffusivity in the system, but instead to dependably transport it to an extraction process where it can be isolated and removed in a controlled manner, thus reducing tritium releases to the environment to a reasonably low level (a reasonable target is the release rate that occurs from typical PWRs).

3.1 Choices of Coolant/Working Fluid

The choice of salt coolants (for the primary and intermediate loops) and working fluid (for the power conversion cycle) can affect the mobility of tritium in the fluid systems. Since there are multiple choices for intermediate coolant salts in a FHR, a compromise can be made between the coolant's thermal, fluid flow, neutronic (for the primary coolant only) and chemical properties and its tritium solubility and/or diffusivity. Tritium as T₂, HT and TF has low solubility in the FHR primary salt, flibe. At the high temperatures of an FHR, these gases diffuse readily through the structural alloys. Diffusion therefore occurs through the intermediate heat exchanger (IHX) into the intermediate cooling loop, and then through the power conversion heat exchanger (PCHX) into the power conversion working fluid. As a result, the choice of power-conversion method will directly impact the strategies for tritium control.

3.2 Components

The flow system component design is also important, since tritium can also permeate and diffuse out of metal components at the high operating temperatures of the FHR into the reactor cavity and intermediate loop insulation systems, as well as the power conversion system. Component tritium permeability must be studied with variable temperature, pressure, coolant composition, and component materials. In addition, the effects of specialized coatings such as silicon carbide (SiC) and oxide layers on reducing tritium permeability should be considered. The design goal for components should be to minimize unintentional tritium permeation out of the system in order to increase the tritium collection efficiency (tritium collected / tritium produced) and reduce the cost of the tritium separation process. Special attention must be paid to the IHX and PCHX heat exchanger designs because the heat exchangers have very large surface areas and are the primary pathway for the tritium to migrate from one loop to another loop, so heat exchangers effectively become the primary tritium source for the intermediate and power-conversion loops.

3.3 Power Cycles

The three candidate power-conversion cycles for the FHR are: Supercritical Steam (SS) Cycle (Figure 2), Closed Brayton (CB) Cycle (Figure 3), and Open Brayton (OB) Cycle (Figure 4). The SS Cycle operates at high temperature and pressure (375 C, 22.06 MPa), has a thermal efficiency of approximately 45%, and utilizes existing technologies already in use in supercritical coal plants; however, tritium is water-soluble and contamination is highly probable.

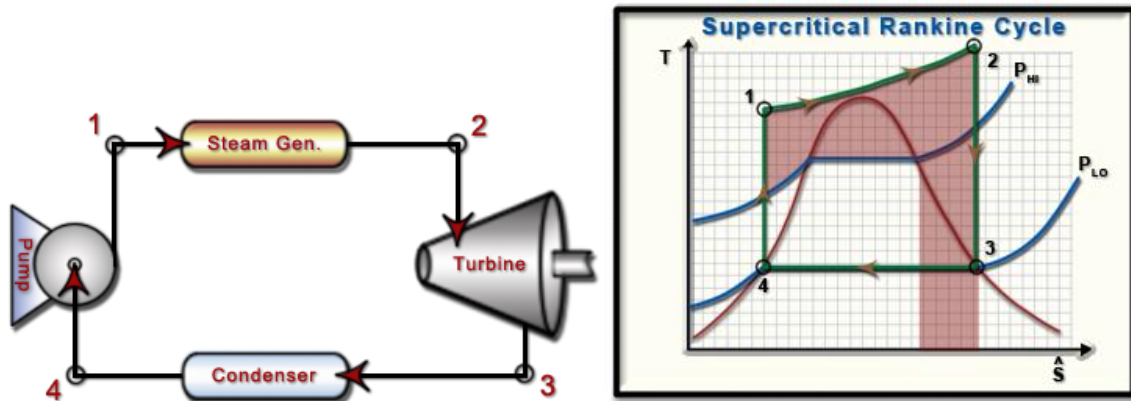


Fig. 2 The Supercritical Steam (SS) Cycle is a classic Rankine Cycle capable of achieving high efficiencies at higher temperatures and pressures. [2]

Options for closed gas Brayton cycles include multiple reheat cycles using helium or nitrogen as working fluids [17], as well as supercritical carbon dioxide cycles. For the CB Cycle, waste heat is rejected to cooling water through a low-temperature heat exchanger, so the diffusivity of tritium is very low and losses remain very small. Despite the benefit of simplified tritium control, these closed cycles remain technically immature and are still under development

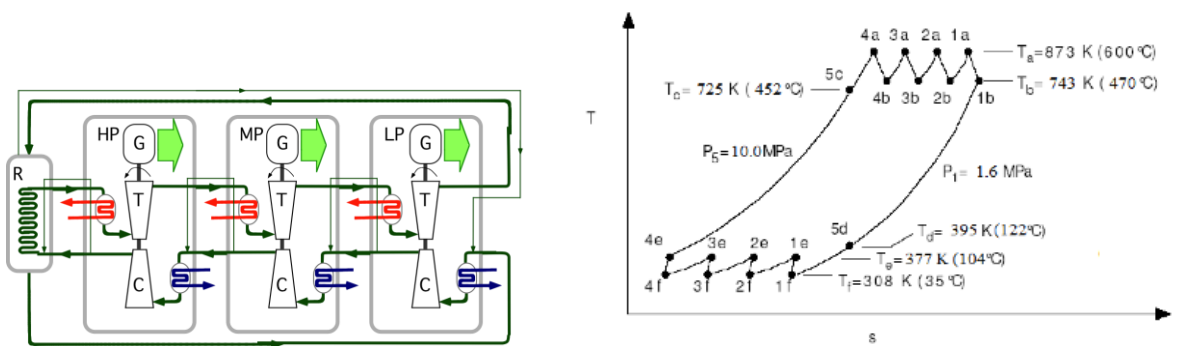


Fig. 3 The Closed Brayton (CB) Cycle cycles through isentropic compression, constant pressure heat addition, isentropic expansion, and constant pressure heat rejection.

The third power-conversion cycle candidate, the OB Cycle, has been widely used in jet engines and gas turbines and can achieve high efficiencies in a combined cycle; however,

the direct heating of ambient air necessitates highly effective tritium recovery to prevent excessive releases.

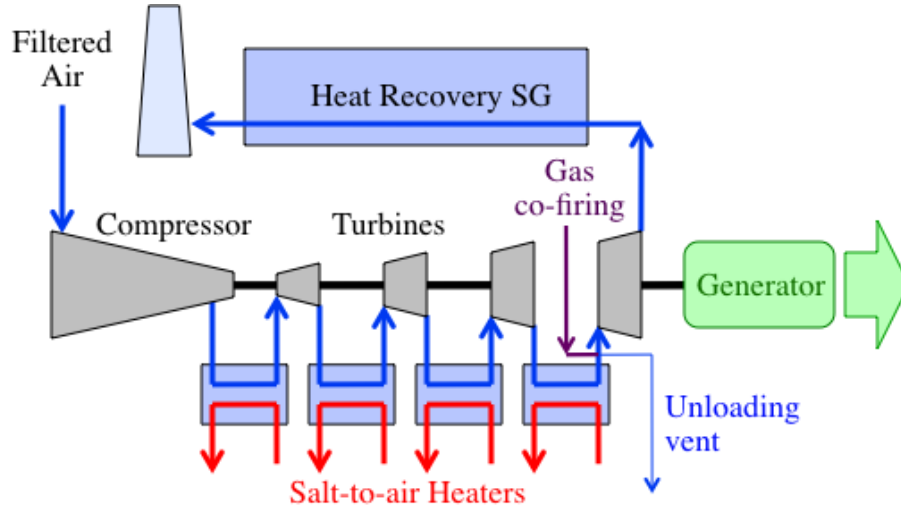


Fig. 4 The Open Brayton (OB) Combined Cycle uses a conventional air compressor, combined with multiple stages of heating and expansion.

3.4 Tritium Transport Model

MATLAB results for mass transfer for each power cycle. Several operating conditions considered. First, the tritium source is assumed to be produced at a constant rate, which was obtained from the MCNP simulation. The tritium production rate, which for a 900 MWth, 410 MWe FHR is calculated to be 7.8603×10^{15} tritium per second from MCNP, is used in the MATLAB model as a steady source. Then, this system is considered to be operating at the temperature around 650°C. Moreover, the volumes of the primary and secondary coolants are assumed to be 15 m³ and 10 m³, respectively. The surface area of both heat exchangers, Intermediate Heat Exchanger (IHx) and Power Conversion Heat Exchanger (PCHX), are assumed to be 1200 m² in this MATLAB model.

With assuming the forced convection allows rapid mixing, the concentrations of tritium in both coolants are considered to be uniform. Thus, a well-mixed control volume approximation can be used in this model. The mass of the tritium in each loop can be predicted as a function of time t as below,

$$m_1(t) = m_p + m_1(t - 1) - S \cdot j_{12}(t) \quad (7)$$

$$m_2(t) = m_2(t - 1) + S(j_{12}(t) - j_{23}(t)) \quad (8)$$

$$m_3(t) = m_3(t - 1) + S \cdot j_{23}(t) \quad (9)$$

where m_1 is the mass of the tritium in the primary coolant, m_2 is the mass of the tritium in the intermediate coolant, m_2 is the tritium production rate from the source (from MCNP), S is the surface area of the both heat exchangers, j_{12} is the tritium flux

through the IHX, j_{23} is the tritium flux through the PCHX, and m_3 is the total amount of tritium permeates through the system into the power conversion fluid.

In the calculation of the tritium flux in each heat exchanger, the diffusion in the heat exchanger alloy is assumed to be the limited regime, which means that the permeation flux cannot be reduced by the interactions of tritium molecular gas with the alloy and the interactions of dissolved tritium in liquid. Then, the tritium flux can be calculated as,

$$j_{12} = \frac{K(\sqrt{P_1} - \sqrt{P_2})}{e} \quad (10)$$

where j_{12} is the tritium flux from station 1 to station 2, K is the permeability of the alloy that used for the heat exchangers, P_1 and P_2 are the partial pressures of the tritium in each station, and e is the effective thickness of the heat exchanger. K depends on the temperature range in which the alloy is used and the alloy that is used. In this model, the permeability of the alloy is chosen for the temperature range close to 650°C. For this model, e is used as 1.6mm for both heat exchangers.

It is possible to coat alloy surfaces with materials such as silicon carbide [6] and metal oxides to significantly (10-400x) reduce tritium permeation rates, with particularly good performance being observed for aluminum oxide layers [3]. This thin layer on the surface of the heat exchangers can result in a surface-limited regime, which means that tritium transport is limited by the physicochemical reactions of adsorption and recombination occurring at the surface of the alloy rather than by the interstitial diffusion. Thus a new parameter, permeation reduction factor (PRF), which measures the relative reduction in tritium permeability compared to the bare-metal case, is needed to add to the previous tritium flux calculation,

$$j_{12} = \frac{K(\sqrt{P_1} - \sqrt{P_2})}{PRF \times e} \quad (11)$$

Depending on the salt that is used in the secondary coolant, the solubility of the tritium in the salt can be determined. As a result, the partial pressure at each coolant can be determined by,

$$P_1 = \frac{m_1}{V_1 \times Sol} \quad (12)$$

where P_1 is the partial pressure in station 1, m_1 is the mass of the tritium in this station, Sol is the solubility of the salt which depends on the operating temperature. The solubility of the salt is also chosen for the system to be operating at 650°C.

Tables 1 and 2 provide parameters for use in an Arrhenius-type relation to derive the relevant quantity:

$$k = K_0 \times e^{\left(\frac{E_0}{RT}\right)} \quad (13)$$

where k is the quantity of interest, K_0 is the pre-exponential factor, E_0 is the activation energy, R is the molar gas constant, and T is the temperature in Kelvin.

Table 1 High-temperature alloy tritium permeability correlations [18]

High-temperature alloy	Pre-exponential factor, K_0 ($m^3(STP)m^{-1}s^{-1}Pa^{-0.5}$)	Activation energy, E_0 ($kJ \cdot mol^{-1}$)	Permeability at 650°C, P ($mol \cdot m^{-1}s^{-1}Pa^{-0.5}$)
Incoloy-800	2.31×10^{-8}	74.1	1.48×10^{-12}
Hastelloy-N	2.59×10^{-8}	77.99	9.99×10^{-13}
Hastelloy-X	5.62×10^{-9}	58.2	2.86×10^{-12}
Hastelloy-XR	1.0×10^{-8}	67.2	1.57×10^{-12}

Table 2 Fluoride salt tritium solubility correlations

Salt	Pre-exponential factor, K_0 ($m^3(STP)m^{-1}s^{-1}Pa^{-0.5}$)	Activation energy, E_0 ($kJ \cdot mol^{-1}$)	Solubility at 650°C, Sol ($mol \cdot m^{-1}s^{-1}Pa^{-0.5}$)
Flibe [4]	7.892×10^{-2}	35.4	7.83×10^{-4}
Flinak [8]	3.98×10^{-7}	-34.4	3.52×10^{-5}

Under different conditions, the time that takes the tritium flux through the PCHX to approach the same value as the tritium source production rate varies. Using the MATLAB code, the tritium flux through the PCHX is compared with the tritium source production rate as the time changes with testing different alloys (Figure 5), PRF (Figure 6), or salts (Figure 7).

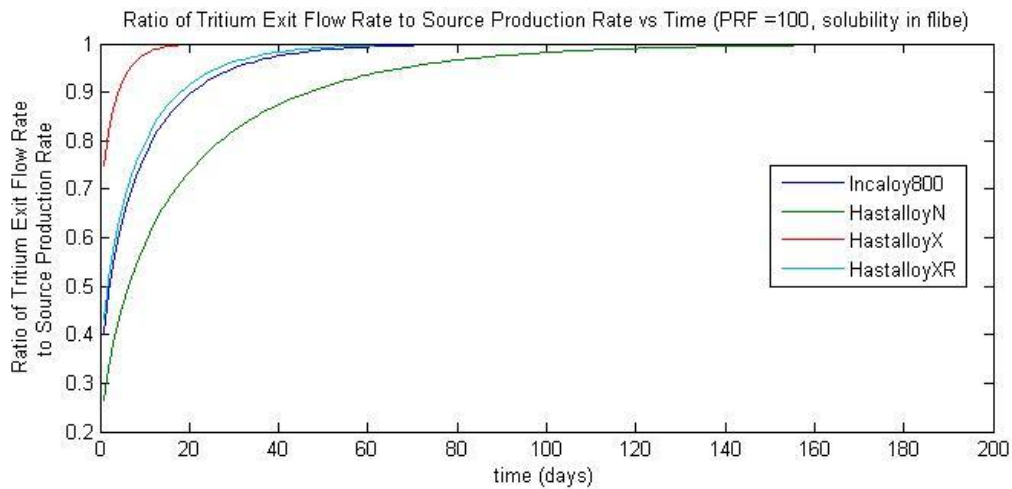


Fig. 5 By setting PRF as 100 and using flibe in the secondary coolant, ratio of the tritium leaving through the PCHX to source production rate is shown for different PHX alloys. The time from longest to shortest for each alloy to reach 1-to-1 ratio is Hastelloy N, Incoloy 800, Hastelloy XR, then Hastelloy X.

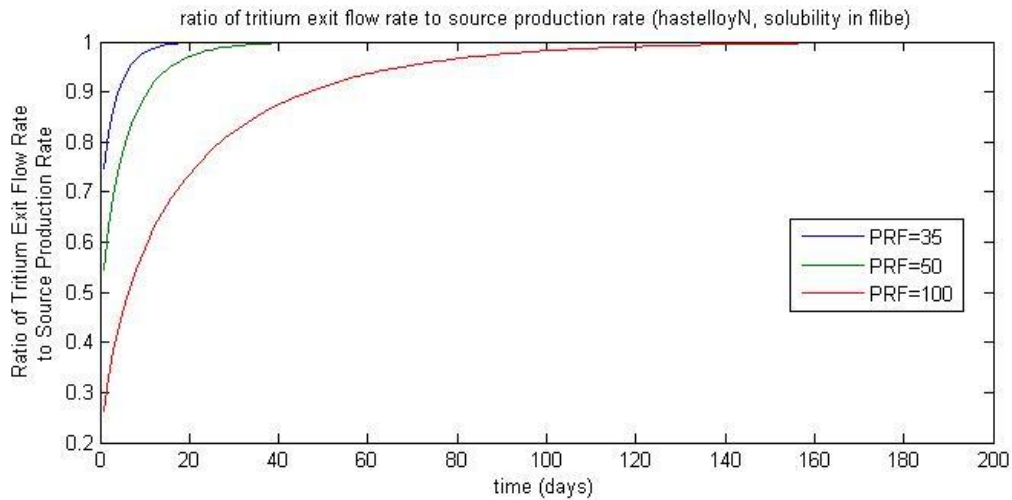


Fig. 6 With using Hastelloy N for the heat exchangers and using flibe in the secondary coolant, ratio of the tritium leaving through the PHX to source production rate vs time comparing with different PRF is shown as above. The time that takes longest to reach 1-to-1 ratio is the one with the largest PRF.

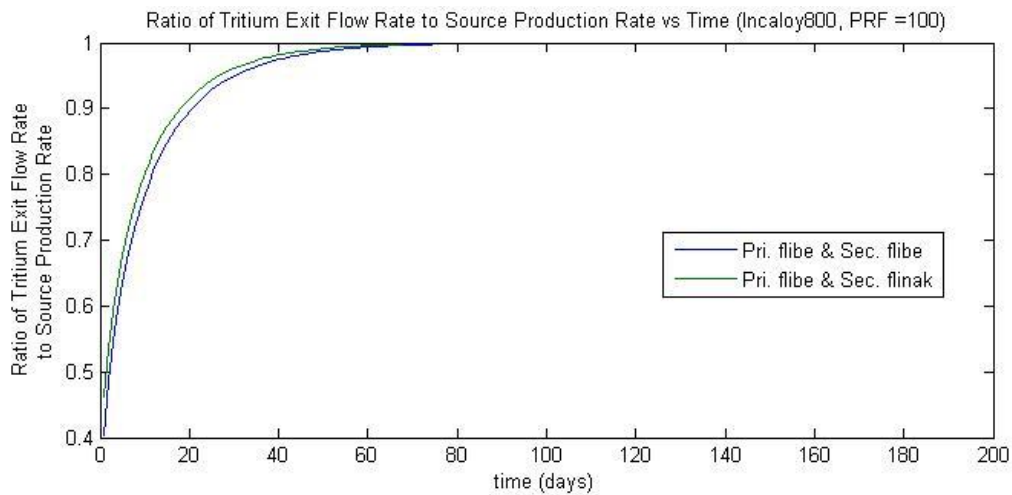


Fig. 7 With setting PRF as 100 and using Incaloy 800 for the heat exchangers, ratio of the tritium leaving through the PHX to source production rate vs time comparing with using either flibe or flinak in the secondary coolant is shown as above. The longest time that takes the ratio to reach 1-to-1 is the one using flibe.

4.0 TRITIUM PROCESSING

Recovery of tritium in PWRs is currently not cost-effective since tritium is in such low concentrations in wastewater and in air discharges (tritium accumulates in the spent fuel pool during refueling, and is released primarily in liquid blow-down from the pool, and from evaporation into air that the ventilation system subsequently discharges to the plant stack). Due to the far larger production of tritium in CANDU reactors, Canada

currently has a tritium recovery program at Darlington that recovers approximately 1.5 kg of tritium every year from 17 operating CANDU reactors [5].

4.1 Dose Restrictions

The Nuclear Regulatory Commission (NRC) has a 3 mrem/yr target for tritium exposure to the public [12]. On the other hand, the US Environmental Protection Agency (EPA) regulation states that concentrations of tritium in drinking water are not to exceed 740 Bq/L; said concentration would equate to 13 $\mu\text{Sv/yr}$ = 1.3 mrem/yr per person. The concentration should actually be about 2253 Bq/L which corresponds to 40 $\mu\text{Sv/yr}$ [16]. This value can be compared to the 620 mrem average annual dose to a United States citizen [12]. In 2005, there were several reports of localized groundwater tritium contamination significantly above EPA levels; however, the contamination has not involved drinking water wells and there have been no adverse health effects observed [14]. Along these lines, tritium remains primarily a legal and public perception issue for operators.

For the open air cycle, the maximum possible tritium concentration in the air turbine exhaust can be estimated from the tritium generation rate and the air flow rate through the turbine. It is expected that the dominating pathway for tritium dispersion to the environment will be diffusion through the heat exchangers into the turbine air streams. Since the tritium release rate will equilibrate with the generation rate within a few months after startup, the tritium concentration in the effluent air stream can be estimated by dividing the steady-state tritium generation rate by the air flow rate:

$${}^3\text{H conc.} \left[\frac{\text{pCi}}{\text{m}^3} \right] = {}^3\text{H gen.} \left[\frac{\text{pCi}}{\text{MW}_{th}\cdot\text{s}} \right] \times \frac{1}{\text{Air flow} \left[\frac{\text{MW}_{th}\cdot\text{s}}{\text{kg}} \right]} \times \text{Air Density} \left[\frac{\text{kg}}{\text{m}^3} \right] \quad (14)$$

Using representative values for some Brayton cycle turbine designs currently under consideration, the resulting ${}^3\text{H}$ concentration will be on the order of 2.5 $\mu\text{Ci/m}^3$. In 10CFR20 Appendix B, the NRC establishes a baseline tritium release limit of 0.1 $\mu\text{Ci/m}^3$ in air effluents [15], which is expected to produce a total effective dose equivalent of 50 mrem if inhaled continuously over the course of a year [11]. Comparison of the representative concentration estimate to the NRC value implies a total effective dose rate of 1.25 rem per year for an individual breathing air directly from the plant stack, or approximately 3.5 mrem per day. This dose rate is approximately double the total average annual dose in the United States. While considerable dilution occurs during transport to the site boundary, the fact that the total tritium production from FHRs is approximately two orders of magnitude greater than PWRs suggests that doses at the site boundary would likewise be some two orders of magnitude greater than for PWRs. This motivates the need for a tritium control system to extract tritium from the secondary salt and process it for safe use or disposal.

4.2 Helium Sparging

A possible method of extracting the tritium produced in an FHR core is to use helium sparging. Helium can be injected into the stream using a multiple slot disperser in order to absorb the tritium produced in the core. The tritium is then allowed to diffuse from the

stream into the bubbles formed by the helium. The amount of tritium stripped from the stream can be calculated by estimating the mass transfer coefficients for the bubbles, compared to the mass transfer coefficients for the PHX. The stream containing the helium and tritium bubbles can be subjected to swirling flow, which would allow bubbles to concentrate into the middle of the pipe to be extracted. The helium can then be separated and the tritium recovered from the helium. As shown in Figure 8, the rate of injection of helium can be controlled to maintain a constant level in a volume control tank, so that the volume fraction of bubbles in the loop is maintained constant.

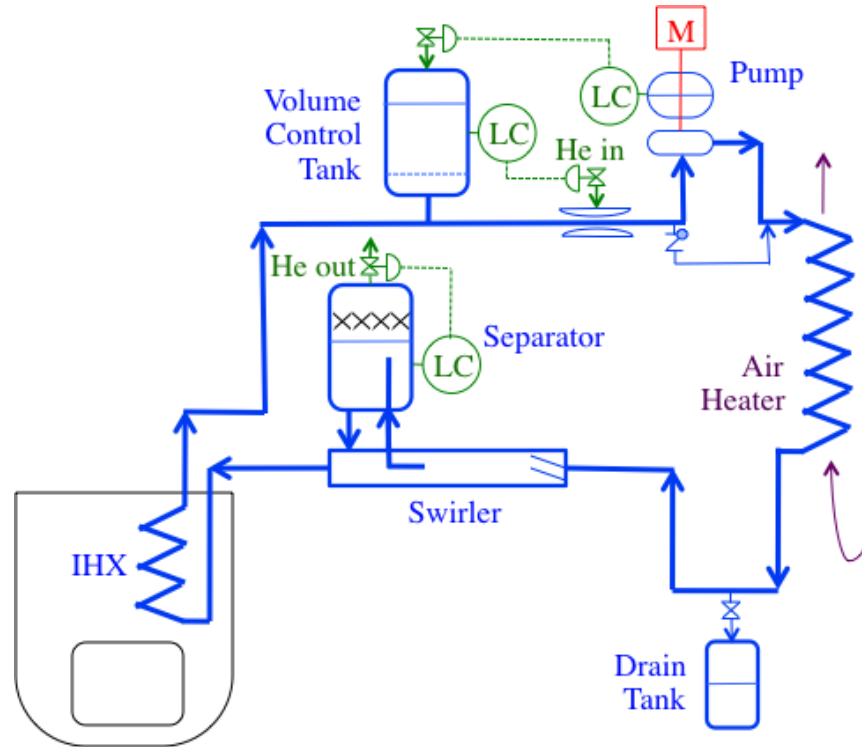


Fig. 8 Schematic diagram of the intermediate-loop helium sparging system, showing volume control, injection, swirler and separating systems for injecting the helium and recovering helium and tritium.

The main challenge in making this an effective method of extraction is the competing mass transfer of tritium through the interface of the helium bubbles and the wall of the heat exchangers. In order to achieve significant extraction of tritium in the bubbles, the surface area of the bubbles must be comparable to the surface area of the heat exchangers, which is about 1200 m^2 . In addition, the volume fraction of the bubbles in the salt should be less than 5%. If the bubbles are injected in a pipe that is 40 meters long with a diameter of 0.30 meters, the diameter of the bubble can be calculated to be around 1 mm.

The non-dimensional governing equations for the injection of these bubbles involve the Froude, Weber, and Reynolds numbers, which are shown below.

$$Fr = \frac{u^2}{gD} \quad (15)$$

$$We = \frac{\rho u^2 d}{\sigma} \quad (16)$$

$$Re = \frac{\rho u D}{\mu} = \frac{u D}{\nu} \quad (17)$$

In the equations, u represents the fluid velocity, ρ the density of the fluid carrying the bubbles, d the diameter of the bubble, D the diameter of the pipe, σ the surface tension of the fluid, and ν the kinematic viscosity of the fluid.

To determine the appropriate slot width needed to generate bubbles of this size, a correlation of bubble volume with Froude and Weber numbers was used [9]:

$$V^* = \frac{V_B g}{(uw)^2} = 26.2 \left(\frac{\rho_l}{\rho_g} \right)^{0.19} \left(Fr^{\frac{4}{3}} We \right)^{-\frac{3}{10}} \quad (18)$$

In this equation, V_B represents the volume of the bubble, w the slot width, ρ_l the density of the fluid, and ρ_g the density of the gas in the bubble.

In order to create a representative model, these numbers must be matched as close as possible to the conditions of the reactor. This is accomplished by first setting the diameter of the bubbles and the desired fluid velocity. Afterward, the Froude and Weber numbers are then scaled to the model, keeping fluid velocity constant. The following table shows the possible conditions of the reactor and the proper scaling to the model assuming the model uses water as the moving fluid.

Table 3 Approximate physical properties of the fluid and bubble sizes in the reactor vs. model (intermediate salt surface tension is not known, but a representative value for other salts is given)

Property	Reactor	Model (using room temperature water as fluid)
Bubble Diameter, d	1 mm	1.3 mm
Pipe Diameter, D	30 cm	30 cm
Density of fluid, ρ	1800 kg/m ³	1000 kg/m ³
Surface tension of fluid, σ	0.1 N/m	0.072 N/m
Kinematic viscosity, ν	2×10^{-6} m ² /s	9×10^{-7} m ² /s
Velocity of fluid, u	1 m/s	1 m/s
Froude Number, Fr_D	0.34	0.34
Weber Number, We_D	18	18
Reynolds Number, Re_D	150000	330000
Slot opening width of multiple slot disperser	42.6 μ m	61.8 μ m

As can be seen by the numbers, the bubbles in the model are slightly larger. In addition, the Reynolds numbers did not match as well as the other two numbers, but they both show that they are in the turbulent regime.

5.0 SUMMARY

This report has identified the risks and concerns associated with tritium production in FHRs. These relative risks and concerns were compared to several existing commercial designs, specifically the PWR, BWR, and CANDU reactors. It was illustrated that FHRs produce enough tritium during all stages of life such that release concentrations in the reactor would be above regulated values for effluent releases. In addition, it was shown that oxide layers alone would not be sufficient to reduce tritium permeability to address this issue. As a result, for open air Brayton and for steam cycles a tritium extraction system will be a necessary component of the FHR reactor design. One proposed system for extraction is called a helium sparging system in which the tritium would be absorbed into bubbles of helium injected into the intermediate coolant. After the tritium has diffused, the bubbles would then be collected using a swirler and then further processed to isolate the extracted tritium. A scaled experiment was proposed to investigate the fluid dynamics of the bubble-salt system.

For future work, the scaled experiment for demonstrating the helium sparging system should be performed. Based upon the parameters above, this experiment would serve as a prototype to mimic actual performance in the reactor. Upon review of the demonstrated feasibility of the design, the overall practicality of a helium sparging system for tritium extraction would be further reviewed. Specifically, once the fluid dynamics has been well established from the scaled experiment, the mass transfer kinetics of the helium bubbles would need to be determined. By improving the MATLAB computer model, the mass transfer of the system could be worked out to determine whether the helium sparging system will be effective enough for use in the FHR.

In addition, the computer model could be altered to accommodate transient conditions, such as during startup, maintenance work or emergency shutdown. The system must not allow uncontrolled tritium releases or unacceptable doses to plant workers or the public, even under extreme emergency conditions. Analysis of tritium production and transport must take into account various stages of equipment startup, shutdown and/or failure in order to ensure this design goal is met. Additionally, the risk of pump cavitation from rogue/stray sparging bubbles should be addressed.

There is the possibility that other methods for tritium removal exist, such as chemical separation. It would be wise to investigate the applicability of alternative tritium removal strategies to the FHR in an effort to increase effectiveness and reduce cost and complexity.

6.0 REFERENCES

1. Bardet, P. et al. "Design, Analysis and Development of the Modular PB-AHTR." *Proceedings of the 2008 International Congress on Advances in Nuclear Power Plants* (2008): 161-78. Print.
2. B-Cubed. "The Supercritical Rankine Cycle." *LearnThermo.com*. 2006. Web. 04 May 2012. <http://www.learnthermo.com/T1-tutorial/ch09/lesson-C/pg04.php>.
3. Bell, J. T., J. D. Redman, and H. P. Bittner. "Tritium Permeation through Clean Incoloy 800 and Sanicro 31 Alloys and through Steam Oxidized Incoloy 800." *Metallurgical Transactions A* 11.5 (1980): 775-82. Print.
4. Calderoni, P., P. Sharpe, M. Hara, and Y. Oya. "Measurement of Tritium Permeation in Flibe (2LiF–BeF₂)." *Fusion Engineering and Design* 83.7-9 (2008): 1331-334. Print.
5. Canadian Nuclear Safety Commission. *Evaluation of Facilities Handling Tritium*. Rep. no. INFO-0796. Canadian Nuclear Safety Commission, 4 Mar. 2010. Web. 4 May 2012. http://nuclearsafety.gc.ca/eng/readingroom/healthstudies/tritium/Evaluation_of_facilities_handling_tritium_info-0796_e.pdf.
6. Causey, R. "The Use of Silicon Carbide as a Tritium Permeation Barrier." *Journal of Nuclear Materials* 220-222 (1995): 823-26. *ScienceDirect.com*. Elsevier B.V., 20 Jan. 2000. Web. 5 May 2012. <http://www.sciencedirect.com/science/article/pii/0022311594006237>.
7. Cisneros, A. et al. "Pebble Fuel Design for the PB-FHR." *Proceedings of the 2012 International Congress on Advances in Nuclear Power Plants* (2012). Print.
8. Fukada, S., and A. Morisaki. "Hydrogen Permeability through a Mixed Molten Salt of LiF, NaF and KF (Flinak) as a Heat-transfer Fluid." *Journal of Nuclear Materials* 358.2-3 (2006): 235-42. Print.
9. Harris, R., K. Ng, and A. Wraith. "Spargers for Controlled Bubble Size by Means of the Multiple Slot Dispenser (MSD)." *Chemical Engineering Science* 60.11 (2005): 3111-115. Print.
10. KAERI. "3H B- DECAY." *atom.kaeri.re.kr*. Korea Atomic Energy Research Institute. Web. 05 May 2012. <http://atom.kaeri.re.kr/cgi-bin/decay?H-3%20B->.
11. NRC. "Appendix B to Part 20-Annual Limits on Intake (ALIs) and Derived Air Concentrations (DACs) of Radionuclides for Occupational Exposure; Effluent Concentrations; Concentrations for Release to Sewerage." *Nrc.gov*. Nuclear Regulatory Commission, 12 Apr. 2012. Web. 05 May 2012. <http://www.nrc.gov/reading-rm/doc-collections/cfr/part020/part020-appb.html>.
12. NRC. "Backgrounder on Tritium, Radiation Protection Limits, and Drinking Water Standards." *Nrc.gov*. Nuclear Regulatory Commission, 29 Mar. 2012. Web. 04 May 2012. <http://www.nrc.gov/reading-rm/doc-collections/fact-sheets/tritium-radiation-fs.html>.
13. NRC. "Frequently Asked Questions About Liquid Radioactive Releases." *Nrc.gov*. Nuclear Regulatory Commission, 12 Mar. 2011. Web. 04 May 2012. <http://www.nrc.gov/reactors/operating/ops-experience/tritium/faqs.html>.

14. NRC. "Groundwater Contamination (Tritium) at Nuclear Plants." *Nrc.gov*. Nuclear Regulatory Commission, 29 Mar. 2012. Web. 05 May 2012.
<http://www.nrc.gov/reactors/operating/ops-experience/grndwtr-contam-tritium.html>.
15. NRC. "Hydrogen-3." *Nrc.gov*. Nuclear Regulatory Commission, 12 Apr. 2012. Web. 05 May 2012. <http://www.nrc.gov/reading-rm/doc-collections/cfr/part020/appb/hydrogen-3.html>.
16. Osborne, Richard. *Review of the Greenpeace Report: "Tritium Hazard Report: Pollution and Radiation Risk from Canadian Nuclear Facilities"*. Rep. Canadian Nuclear Association, Aug. 2007. Web. 5 May 2012.
http://www.cna.ca/english/pdf/studies/ReviewofGreenpeacereport_Final.pdf.
17. Peterson, Per F. "Multiple-Reheat Brayton Cycles for Nuclear Power Conversion With Molten Coolants." *Nuclear Technology* 144.3 (2003): 279-88. Print.
18. Takeda, T., J. Iwatsuki, and Y. Inagaki. "Permeability of Hydrogen and Deuterium of Hastelloy XR." *Journal of Nuclear Materials* 326.1 (2004): 47-58. Print.

7.0 APPENDIX

7.1 MATLAB Code

```
%% VHTR Model
clc;
clear;

T = 650 + 273; %Kelvin, Operating temperature
R = 8.314; %Joules/(mol*K), Molar gas constant
Na = 6.02e23; %Avogadro's number

%%%%%%%%%%%%%%%%%%%%%%%%%%%%%%%%%%%%%%%%%%%%%%%%%%%%%%%%%%%%%%%%%%%%%%%%%
%Different Test case properties%%%%%%%%%%%%%%%%%%%%%%%%%%%%%%%%%%%%%%%%%%%%%%%%%%%%%%%%%%%%%%%%%%%%%%%%%
%Alloy properties
E_incoloy800 = 74.1e3; %J/mol, activation energy of alloy permeability
P_incoloy800 = 2.31e-8; %m^3(STP)/(m*s*Pa^(.5)), pre-exponential
factor for alloy permeability

E_incoloy800_2 = 74.1e3; %J/mol, activation energy of alloy
permeability
P_incoloy800_2 = 9.77e-9; %m^3(STP)/(m*s*Pa^(.5)), pre-exponential
factor for alloy permeability

E_hastelloyN = 77.99e3; %J/mol, activation energy of alloy permeability
P_hastelloyN = 2.59e-8; %m^3(STP)/(m*s*Pa^(.5)), pre-exponential
factor for alloy permeability

E_hastelloyX = 58.2e3; %J/mol, activation energy of alloy permeability
P_hastelloyX = 5.62e-9; %m^3(STP)/(m*s*Pa^(.5)), pre-exponential
factor for alloy permeability

E_hastelloyXR = 67.2e3; %J/mol, activation energy of alloy permeability
P_hastelloyXR = 1.0e-8; %m^3(STP)/(m*s*Pa^(.5)), pre-exponential
factor for alloy permeability

%Salt properties
E_flibe = 35.403e3; %J/mol, activation energy of salt solubility
P_flibe = 7.892e-2; %mol/(m^3*Pa), pre-exponential factor for salt
solubility

E_flinak = -34.4e3; %J/mol, activation energy of salt solubility
P_flinak = 3.98e-7; %mol/(m^3*Pa), pre-exponential factor for salt
solubility
%%%%%%%%%%%%%%%%%%%%%%%%%%%%%%%%%%%%%%%%%%%%%%%%%%%%%%%%%%%%%%%%%%%%%%%%%

%%%Source term%%%%%%%%%%%%%%%%%%%%%%%%%%%%%%%%%%%%%%%%%%%%%%%%%%%%%%%%%%%%%%%%%%%%%%%%%
mcnp_source = 7.86403E+15/Na; %moles/second, tritium steady-state
source from mcnp
%%%%%%%%%%%%%%%%%%%%%%%%%%%%%%%%%%%%%%%%%%%%%%%%%%%%%%%%%%%%%%%%%%%%%%%%%
```

```

%%%Exchanger properties%%%%%%%%
S1=1200; %m^2 (surface area of the exchangers)
Kxrt=P_incoloy800*exp(-E_incoloy800/(R*T)); %mol.m-1.s-1.Pa-0.5
(tritium permeability in HX alloy @ T)
Slshprim=P_flibe*exp(-E_flibe/(R*T)); %mol.m-3.Pa-1 (tritium solubility
in salt @ T for primary loop)
solsec=P_flinak*exp(-E_flinak/(R*T)); %mol.m-3.Pa-1 (tritium solubility
in salt @ T for secondary loop)
V1=15; %m^3 (primary coolant volume)
V2 = 4; %m^3 (secondary coolant volume)
PRF=100;% Permeation Reduction Factors
thickness = 1.6*10^(-3); %m, characteristic thickness of alloy
%%%%%%%%%%%%%%%%%%%%%%%%
%%%%%%%%Timesteps (seconds)
d=600; %number of days of calculation
n=24*3600; %number of timesteps per day
stepsize = 1; %size of timestep (seconds)
%%Reminder: stepsize*n should equal 1 day!
%%%%%%%%%%%%%%%%%%%%%%%%

%%intial conditions%%%
ms1(1:d)=0;
ms2(1:d)=0;
ms3(1:d)=0;
ps1(1:d)=0;
ps2(1:d)=0;
js1(1:d)=0;
js2(1:d)=0;
js3(1:d)=0; %*****
m1=0.001; %initial moles of T in primary coolant
m2=0;
m3=0;
p1=0;
p2=0;
j1=0;
j2=0;
%%%%%%%%

%Calculation starts here
x1=V1*Slshprim;
x2=V2*solsec;
x3=Kxrt/(PRF*thickness); %permeability/PRF

for i=1:d %days of calculation.
for j=1:n %timestep within day (seconds)
%mt=m0*(exp(x1*((n1-1)*(i-2)+j-2))-exp(x1*((n1-1)*(i-2)+j-1))); %g
(tritium production)
mt = mcnp_source*stepsize; %moles, source term
p1=m1/x1; %Pa (t2 partial pressure in the primary coolant)
p2=m2/x2; %Pa (t2 partial pressure in the secondary coolant)
sqrt_p2=sqrt(p2);
j1=(sqrt(p1)-sqrt_p2)*x3; %mol.m-2.s-1 (t flux through the IHX)
j2=sqrt_p2*x3; %mol.m-2.s-1 (t flux through the PHX)

```

```
m3=m3+stepsize*S1*j2; %g (t power conversion side)
m2=m2+stepsize*S1*(j1-j2); %g (t secondary coolant)
m1=m1+mt-stepsize*S1*j1; %g (t primary coolant)
end
ms1(i)=m1;
ms2(i)=m2;
ms3(i)=m3;
ps1(i)=p1;
ps2(i)=p2;
js1(i)=j1;
js2(i)=j2;
end

figure; plot(1:1:d,(js2*S1/mcnp_source)); xlabel('time (days)');
title('ratio of tritium exit flow rate to source production rate');
%%plots ratio of tritium exit flow rate to source production rate
```